JOURNAL OF CATALYSIS **178,** 1–13 (1998)
ARTICLE NO. CA982154

Aromatization of *n*-Heptane on Pt/Alkali or Alkali-Earth Exchanged Beta Zeolite Catalysts: Catalyst Deactivation and Regeneration

F. J. Maldonado-Hódar, M. F. Ribeiro,[1] J. M. Silva, A. P. Antunes, and F. R. Ribeiro

Departamento de Engenharia Química, Instituto Superior Técnico, Avenida Rovisco Pais 1096, Lisboa Codex, Portugal

Received January 21, 1997; revised May 14, 1998; accepted May 18, 1998

Two series of supports and catalysts were prepared exchanging β zeolite with alkali or alkali-earth cations. The influence of the exchanged cation (M = Na, K, Rb, Cs, Mg, Ba) on the catalytic behaviour of Pt/Mβ catalyst in *n*-heptane reactions was studied. Platinum was introduced into the supports by ionic exchange. The supports and Pt catalysts were chemical and structurally characterized by different techniques (AA, ICP, XRD, ammonia TPD, cyclohexane adsorption, H_2-TPR, etc.). The acidity and adsorption capacity decrease as the cation size increases. In the case of alkali cations, the catalytic activity of the support is negligible. However, greater acidity and stronger acid sites present on alkali-earth supports provide a high catalytic activity. The deactivation rate and the amount of coke determined by TG are related. The nature of the coke was discussed on the basis of DSC results obtained during the coke burning. Coke deposited on alkali and alkali-earth Mβ zeolite during the *n*-heptane transformation becomes progressively more stable as the support acidity and the time on stream increase. The localization of Pt particles and their proximity to the acid sites influence the coke composition and its removal. The regeneration of Pt/Kβ was performed and the results showed that the catalyst fully recovers its catalytic behaviour.

Key Words: **beta zeolite; platinum; alkali and alkali-earth cations; *n*-heptane reactions; catalyst deactivation; coke deposition.**

INTRODUCTION

The formation of coke during hydrocarbon transformation over catalysts has important practical consequences for a growing number of industrial processes (1–6). Coke is a very general word usually assigned to carbonaceous compounds (polyaromatic or nonpolyaromatics) formed during a reaction and it is responsible for catalyst deactivation (7). The deactivation rate depends obviously on the relative rate of formation of these by-products. The deactivating effect of coke is more pronounced when deactivation is due to pore blockage than when it is due to site coverage (8). The catalyst deactivation varies strongly from one catalytic system to another. In the particular case of zeolite catalysts, coke formation has been mainly studied in the context of catalytic cracking, and a number of reviews are available (6–8) which provide a large information about the chemistry of coke formation, techniques for coke characterization, the influence of parameters as pore structure or zeolite acidity, and coke removal or catalyst regeneration.

Over the years, catalytic reforming has been one of the most important industrial processes for the upgrading of naphtas, using bifunctional catalysts formed by a combination of platinum with rhenium or iridium, supported on Al_2O_3 (9). However, since Bernard (10) reported the exceptional catalytic performance of Pt supported on nonacidic KL zeolite, for aromatization of straight-chain paraffins, this catalyst has been largely studied. This catalyst is severely deactivated by trace sulfur impurities but shows a large stability for reforming of desulfurized feed (11). More recently, Iglesia (12) studied the carbon fouling of Pt/KL during heptane reforming concluding that the L zeolite pores inhibit coke formation so that platinum inside the pores remains free of carbon residues.

The catalytic performance of Pt/Hβ catalyst in reforming of different hydrocarbons was studied by Smirniotis *et al.* (13–15). They found that β zeolite catalyst is deactivated more easily than alumina due to the coke build up on the acidic sites (13, 14). Low deactivation was detected for *n*-hexane reactions at 300°C, due to the low yields of cyclic products, but it increased at higher temperatures, when aromatic products appeared. When the reforming of methylcyclopentane and ethylcyclopentane was studied, deactivation was found to be stronger, with the coke formation being greater in the case of ethylcyclopentane (14). The effect of the support acidity was also studied (14, 15). The control of the Brönsted acidity via dealumination minimizes coke formation and hydrocracking, and it results in the preservation of the catalyst activity. Maximum aromatic yield was found for a dealuminated catalyst with a SiO_2/Al_2O_3 molar ratio of 130 and 0.5% Pt (15). With respect to the coke nature, when methylcyclopentane is used as feed, the aromaticity of the soluble coke decreases for more dealuminated β zeolite, indicating that the aromatic coke is preferably deposited on the acidic sites. Zheng *et al.* (16) studied the *n*-hexane aromatization on Pt/β-zeolite exchanged with alkali metals

[1] Corresponding author. E-mail: qfilipa@alfa.ist.utl.pt.

0021-9517/98 $25.00

and found that this catalyst is more resistant to sulfur poisoning than Pt/KL, which is the less acid catalyst and the less severely poisoned catalyst.

However, there is a lack of information about the deactivation of Pt catalysts prepared from zeolites exchanged with different cations. In this work we have been studying the *n*-heptane aromatization on Pt/β-zeolite exchanged with alkali (Na, K, Rb, Cs) and alkali-earth (Mg, Ba) metals. Studies on the influence of the exchanged ion on the catalyst properties and the deactivation/regeneration processes were also performed.

TABLE 1

Composition of the Different Catalysts

Catalyst	Unit-cell composition	Pt (wt%)	S_{BET} ($m^2 g^{-1}$)	d[a] (nm)
Pt(0.5%)/Naβ	$Na_{2.79}H_{1.06}(Al_{3.85}Si_{60.05}O_{128})$	0.52	540	3.8
Pt(0.2%)/Naβ	$Na_{2.79}H_{1.06}(Al_{3.85}Si_{60.05}O_{128})$	0.20	540	1.6
Pt/Kβ	$K_{3.08}H_{0.77}(Al_{3.85}Si_{60.05}O_{128})$	0.38	470	1.8
Pt/Rbβ	$Rb_{3.81}H_{0.04}(Al_{3.85}Si_{60.05}O_{128})$	0.33	n.d.	n.d.
Pt/Csβ	$Cs_{3.54}H_{0.31}(Al_{3.85}Si_{60.05}O_{128})$	0.21	313	1.2
Pt/Mgβ	$Mg_{1.55}H_{0.70}(Al_{3.85}Si_{60.05}O_{128})$	0.50	492	2.1
Pt/Baβ	$Ba_{1.93}(Al_{3.85}Si_{60.05}O_{128})$	0.24	335	1.2

[a] Pt particle size estimated by CO chemisorption.

EXPERIMENTAL

The β zeolite supplied by EXXON, under the form NaHβ, was exchanged twice with a 0.5 *M* $NaNO_3$ solution in order to ensure the greatest possible elimination of protons. The ion exchange process was carried out at 80°C for 2 h, under vigorous stirring, using a ratio volume of solution (mL)/zeolite weight (g) of 70. The dispersion was centrifuged and the solid washed and dried overnight at 110°C. Further, portions of this zeolite form were also exchanged twice with KNO_3, $RbNO_3$, and $CsCH_3COO$, respectively, using the same procedure. All the samples were finally calcined in air flow (3 L/h · g) with the temperature being ramped at a rate of 2°C/min from 25 to 500°C with a hold at 500°C for 2 h. The obtained samples were denominated Naβ, Kβ, Rbβ, and Csβ, respectively. The same procedure using $MgNO_3$ or $BaCH_3COO$ was followed to obtain the alkali-earth exchanged Mgβ and Baβ supports.

Platinum was loaded into the support materials by ion exchange, using $Pt(NH_3)_4(NO_3)_2$ as precursor. The exchange was carried out for 4 h at room temperature and under stirring. The programmed platinum load was 0.5 wt% using a $Pt(NH_3)_4(NO_3)_2$ solution of 400 ppm. After centrifuging and washing, the catalyst was dried for 12 h at 110°C and calcined at 300°C for 2 h under air flow (3 L/h · g).

Pt/KL zeolite was used as reference due to well-known catalytic performance. KL zeolite was supplied by UOP with a SiO_2/Al_2O_3 molar ratio of 6.3. Pt exchange was also carried out under the same conditions and a content of 0.37 wt% was obtained.

Chemical composition of the samples was determined by atomic absorption spectroscopy (AA), inducted coupled plasma spectroscopy (ICP), and energy dispersive X-ray fluorescence (EDX RF). The corresponding unit cell compositions are listed at Table 1. The samples were also characterized by XRD, being the experiments performed in a Rigaku apparatus using the CuKα radiation (Ni filter) at 2°/min.

Textural characteristics of Mβ supports were studied by N_2 adsorption and dynamic cyclohexane adsorption. The N_2 adsorption was carried out in an "Area Meter" of Strölhein Instruments. The samples were outgassed for 4 h at 200°C and 10^{-2} Torr and N_2 was adsorbed at 77 K (liquid N_2 temperature). Dynamic adsorption of cyclohexane was carried out at 90°C using a Setaram TG-DSC92 thermobalance. After pretreatment under N_2 at 500°C for 10 min, the samples were cooled down to 90°C, and after stabilizing the sample weight, the N_2 flow was changed to N_2-cyclohexane flow obtained bubbling N_2 (50 mL/min) in a cyclohexane saturator at 14.6°C.

Temperature-programmed desorption (TPD) of NH_3 was carried out using 150 mg of zeolite sample (Mβ) that was placed in a quartz reactor and heated under He flow (1 mL/s) up to 550°C in order to have a clean catalyst surface; after 1 h at these conditions, the reactor was cooled to the adsorption temperature. The sample was saturated passing a mixture of He/NH_3 (0.2% NH_3) for 4 h at the adsorption temperature (150°C). After purging 30 min with He, NH_3 was desorbed by heating at 10°C/min under the same He flow, with on-line gas analysis performed with a TCD detector of a Shimadzu GC-8A gas chromatograph.

The activity of the support in acid and/or basic reactions was evaluated using *n*-heptane cracking and 1-butene isomerization. The *n*-heptane cracking was performed using the conditions mentioned below for Pt catalysts. The 1-butene isomerization was carried out at 150°C, WHSV = 0.17 h^{-1}, and introducing 1 mL/min of pure 1-butene and 49 mL/min of N_2.

Temperature-programmed reduction (H_2-TPR) experiments were developed following a similar TPD procedure; 80 mg of Pt/Mβ catalyst were pretreated at 200°C for 1 h under Ar flow (1 mL/s) and then cooled to room temperature. The gas was then switched to a 5% H_2/Ar mixture flowing at the same rate. During the TPR experiments, temperature was increased at a rate of 10°C/min and the consumed H_2 was monitored by a TCD detector.

Platinum dispersion was studied by CO chemisorption and transmission electron microscopy (TEM). CO chemisorption isotherms were measured between 0–200 Torr, using a conventional volumetric system at room temperature (25°C). The catalysts were also previously reduced for 2 h at 500°C in H_2 flow and then evacuated at

this temperature to less than 10^{-5} Torr for 2 h. After the first isotherm was measured, the sample was evacuated at 10^{-5} Torr for 30 min and a second isotherm was measured. Following the second isotherm, the sample was again evacuated at 10^{-5} Torr and the volume of the reactor determined with He. The amount of chemisorbed CO was calculated by extrapolating the isotherms to zero pressure and taking the difference between the first and second isotherms. Transmission electron micrographs were recorded on a JEOL microscope (JEM 100 CXII) operating at 100 KV. The samples were prereduced at 500°C under H_2, ground to a fine powder, embedded in an epoxy resin, and sectioned with an ultramicrotome (80–100 nm).

n-Heptane reactions were performed on a continuous-flow reactor. Pt/Mβ catalysts (150 mg) were reduced in situ at 500°C for 5 h. The catalytic behaviour of the different samples was compared at atmospheric pressure, 450°C, $H_2/C_7 = 6$, and WHSV = 15 h^{-1}. Only H_2 acts as a carrier gas, and consequently, the total flow in the reactor varies as a function of the experimental conditions; *n*-C_7 was mixed with the H_2 flow in a prereactor camera heated at 80°C. The purity of *n*-heptane (Merck) was at least 99%, containing less than 0.005% of sulfur, because nothing has been done in order to eliminate it. The reaction products were analysed by on-line gas chromatography with a FID detector and PONA column. Results were reported as conversions calculated as the mole-percent of *n*-heptane reacted.

The coke analyses were performed by thermogravimetry using a Setaram TG-DSC92 thermobalance. Coked samples were heated under air flow with a temperature increase of 10°C/min until 200°C, maintaining this temperature for 1 h. Afterwards, the temperature was increased again with the same heating rate until 800°C. The samples were cooled to room temperature and an additional heating cycle was performed under identical conditions to eliminate any fluid transport effect. The weight loss and heat profiles were obtained by subtraction of the two cycle profiles.

RESULTS AND DISCUSSION

(a) Characterization of Supports and Pt/Mβ Catalysts

β zeolite was exchanged with alkali (Na, K, Rb, Cs) or alkali-earth metals (Mg, Ba). The ionic exchange process induces textural and chemical changes on β zeolite, factors that influence strongly the coke deposition on the catalyst (6, 7).

NH_3 TPD spectra of Mβ zeolites (M = Na, K, Cs, Mg, Ba) are presented in Fig. 1. An intense low temperature peak (250–300°C) appears for all samples, except for Csβ. The high temperature peak (550–600°C) indicating the existence of stronger acid sites, also appears for all supports, showing great differences between them. Alkali-earth exchanged supports are more acid than alkali exchanged ones, the differences in amount being greater for stronger acid

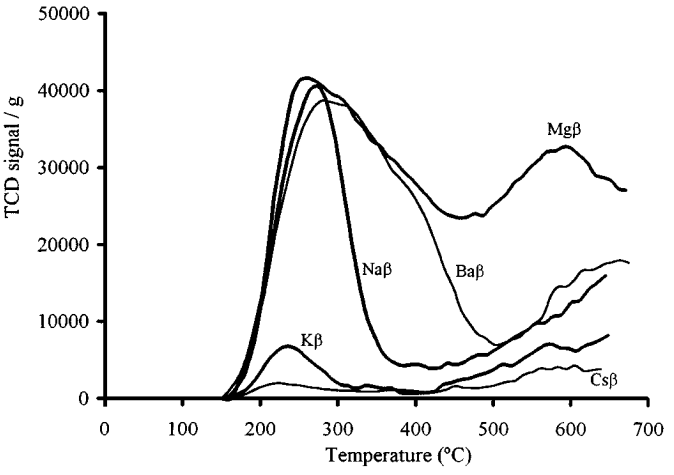

FIG. 1. Evolution of the NH_3 TPD profiles for alkali and alkali-earth β zeolites.

sites. Csβ zeolite presents the lowest acidity of both catalyst series, decreasing this parameter strongly with respect to Naβ zeolite. Between Mgβ and Baβ zeolites the main differences are located in the stronger acid sites.

Figure 2 shows the results obtained by dynamic cyclohexane adsorption. In both series, the cation size influences either adsorption rate or adsorption capacity. Naβ and Mgβ present similar adsorption capacity, the adsorption rate being slightly greater for Mgβ. Csβ shows the slowest adsorption rate and an adsorption capacity quite close to Baβ. KL zeolite shows the highest adsorption rate and the lowest adsorption capacity. We can conclude that simultaneously to the acidity decrease provoked by the exchange of the zeolite with large cations, an important porous blockage takes place. From Table 1 it can be observed that ionic exchange also produced changes in the BET surface area, decreasing from small cations (Na or Mg) to larger ones (Cs and Ba).

The XRD patterns of the different exchanged samples are shown in Fig. 3. All the samples retained the structure of

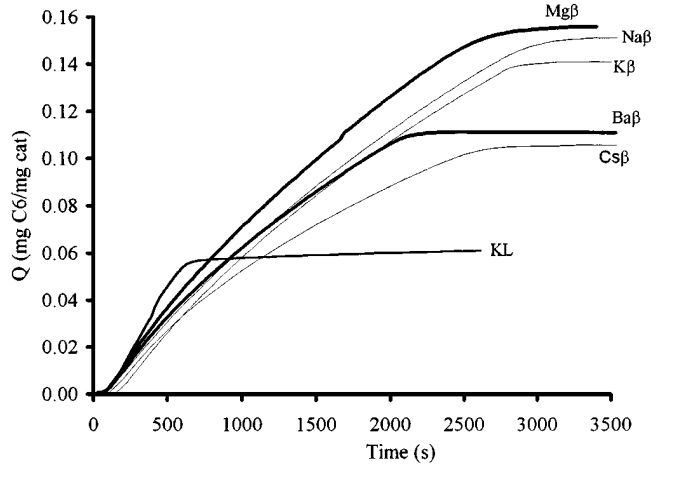

FIG. 2. Adsorption of cyclohexane on Mβ zeolites and KL zeolite.

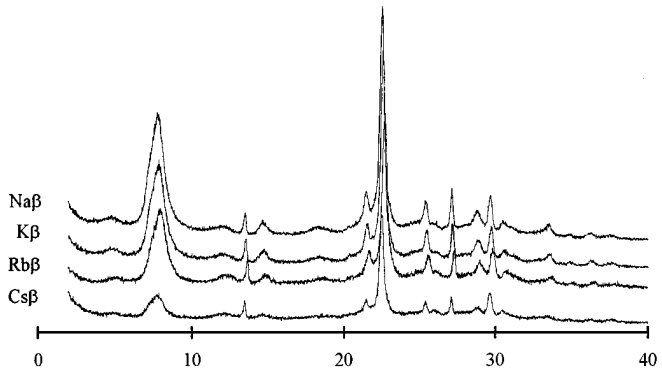

FIG. 3. XRD patterns of alkali exchanged β zeolites.

β zeolite, and no evidence of the presence of another phase was observed. The decrease of intensity observed when the zeolite is exchanged with large cations (Cs and Ba) is due mainly to the different absorption of X-rays by the cation. The crystallinity was determined comparing the area of the most intense diffraction peak ($2\theta = 22.4$), and after correction from the X-ray absorption changes, we found a loss of 7% of crystallinity for the Csβ zeolite. In this case we are assuming that the ionic exchange with large cations produces mainly blockage of porosity, but we do not exclude completely the introduction of some new defects, producing a partial loss of crystallinity. Different works have previously pointed out changes of X ray profiles following some treatments that introduce microstructural defects in the framework structure of β zeolite (13, 17).

The platinum was introduced on the different supports by ionic exchange. Although the programmed Pt loading was similar in all cases (0.5%), only the supports exchanged with the smaller cations attained this concentration, which decreases progressively as the cation size becomes larger (Table 1). This observation is also useful to confirm the increase of blockage of porosity by the bulkier cations, which inhibit the access of Pt amine complexes to the most inner exchange sites.

Hydrogen TPR profiles obtained with Pt/KL, Pt/Naβ, Pt/Csβ, and Pt/Baβ are presented in Fig. 4. For Pt/Naβ only one important peak is observed at high temperature, for Pt/Csβ another important peak is centered about 200°C. TPR profiles obtained with Pt/Csβ and Pt/KL are very similar. In the case of alkali-earth exchanged catalysts similar results were obtained, but the TPR profile for Pt/Baβ also showed two peaks. According to Zheng *et al.* (18) that studied the state of Pt in exchanged β zeolites, the peak about 195°C corresponds to the reduction of Pt^{+2} ions located in the main channels of β-zeolite, and the peak about 430°C corresponds to the reduction of Pt^{+2} ions in some hidden sites. Therefore, it means that in our case, Pt particles are mainly located in the hidden sites and the amount of Pt^{+2} ions located in the most accessible sites (peak at 200°C) clearly increases with the cation size. The presence of bulky cations, such as Cs and Ba, inhibits the diffusion of the platinum amine complexes inside the zeolite and some Pt particles are forced to remain in the mouth of the zeolite pores, or even on the external surface, a bimodal distribution as was described previously being observed for the Pt/KL catalyst (19).

The analysis of TEM data shows good platinum dispersion for all the samples, without significant differences in the particle diameters. For alkali samples, the average particle diameter was about 20 Å, and only Rbβ showed a broader distribution shifted to larger sizes ($d = 45$ Å). Pt/Csβ presents the smallest particle diameters (17 Å), in the same range of that observed for Pt/KL zeolite, and no larger particles were observed. In this particle size distribution we do not take into account the presence of very small (<10 nm) particles that are not visible by TEM. In Pt/Naβ sample, some scarce but larger particles were also observed. CO chemisorption data reported in Table 1 show Pt particle sizes not very different from the ones measured by TEM. However, the trend for decreasing Pt particle sizes from Na to Cs is more evident from chemisorption results.

(b) Catalytic Tests

(b1) Catalytic activity of the supports. The catalytic activity of both supports series on *n*-heptane reactions was evaluated at 450°C, WHSV = 15 h^{-1}, and molar ratio $H_2/C_7 = 6$. When the alkali-exchanged zeolites were tested, only Naβ support (the most acidic support of the series) presented catalytic activity. However, the conversion values are low (about 4% at the reaction beginning) and decrease quickly in such a manner that after a 30-min run, the conversion is lower than 1%. Only cracking products were detected. However, in the case of alkali-earth both Mgβ and Baβ supports presented a high catalytic activity. Figure 5 shows the evolution of the catalytic activity in

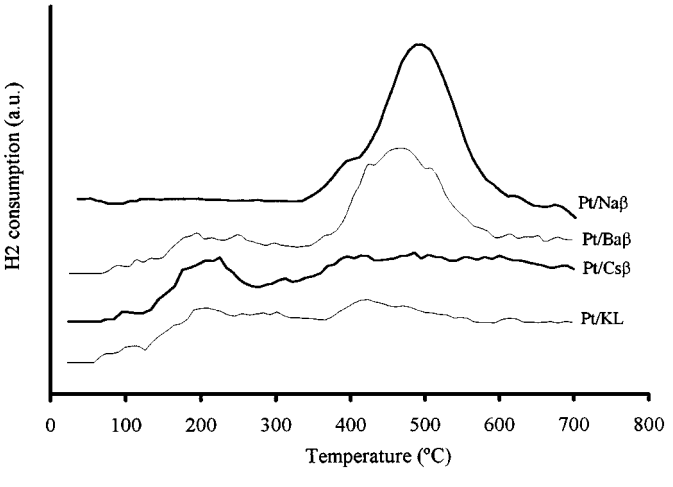

FIG. 4. TPR profiles of Pt/Naβ, Pt/Csβ, Pt/Baβ, and Pt/KL zeolites.

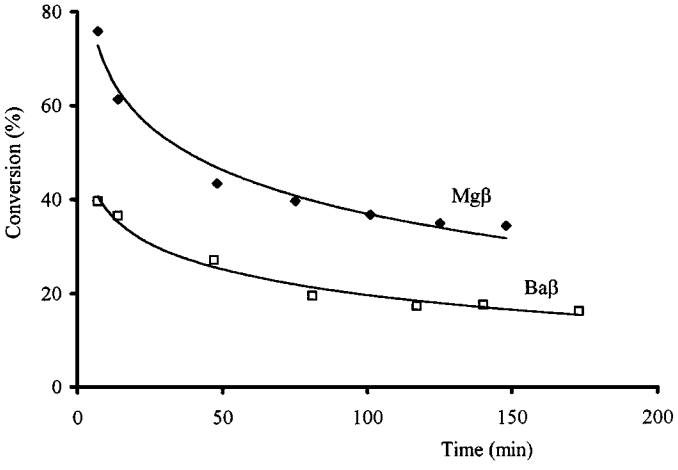

FIG. 5. Catalytic activity of Mgβ and Baβ supports on *n*-heptane reactions at 450°C, WHSV = 15 h^{-1}, and $H_2/C_7 = 6$.

n-heptane reactions of both supports along the reaction time. Mgβ support shows an initial conversion of *n*-heptane close to 80% (the first analysis was always performed after 7 min on stream). The activity of Mgβ support is about two times the Baβ activity. Both supports produced mainly products of cracking, the cracking selectivity being always greater than 99%. Both supports produced practically equimolar amounts of C_3 and C_4's; smaller amounts of C_2, C_5, and C_6 are also observed more significantly at the reaction beginning, while the formation of methane was always negligible. This fact indicates that cracking is mainly due to the hydrocracking process which produces equimolar amounts of C_3 and C_4's although the presence of other cracking products may suggest some dimerization of heptane and posterior cracking (20).

With the purpose to better characterize the different catalytic sites subsisting in the supports, we examined the skeletal isomerization of 1-butene into isobutene and double bond isomerization to *cis*- and *trans*-2-butene. These two types of isomerization occur normally during the transformation of 1-butene at low temperature, but depending of the acidity of the catalysts, the isobutene formation will be favoured, and high *cis/trans* 2-butene ratios are a good indication that the reaction is base catalysed (21). The results shown in Table 2 reveal that both alkali and alkali-earth supports are active for 1-butene isomerization, but Mgβ has strong enough acidity to provide the skeletal isomerization. The *cis/trans* 2-butene ratios observed from the several samples are low and do not evidence significant differences in base properties. As was expected, the Mgβ sample shows the lowest *cis/trans* ratio, but the samples with Cs and Ba that we would suppose more basic only showed slightly higher values.

TABLE 2

Catalytic Data for Mβ Supports for the Isomerization of 1-Butene

Sample	Initial conversion ($t = 7$ min)	Isobutene selectivity	2-Butene *cis/trans* ratio
Naβ	45.3	0.0	1.0
Csβ	21.3	0.0	1.2
Mgβ	96.9	11.2	0.6
Baβ	56.3	0.0	1.1

(b2) Pt/Mβ catalysts performance. Pt/Mβ catalysts were tested with *n*-heptane under the same experimental conditions mentioned above. Our initial purpose was to obtain Pt/Mβ catalysts with low acidity, because acidity is highly undesirable; protons are known to lower selectivity to aromatics and also catalyst stability (10). Taking into account the results previously exposed, showing a very low acidity and activity on alkali/β zeolites, we would expect that platinum in these catalysts, and mainly in Pt/Csβ, could alone catalyse the *n*-heptane transformation. However, we are conscious that, during the activation of platinum, some additional protons can be formed from Pt^{2+} ions (22). Nevertheless this phenomena can happen in all catalysts, its consequences being higher for catalysts containing greater platinum content, such as Pt/Naβ catalyst, whose support had already presented the highest acidic activity. In the case of Pt/alkali-earth Mβ catalysts (M = Mg or Ba) there is no doubt about the participation of platinum, together with acid sites in *n*-heptane reactions. The larger amount of stronger acid sites on alkali-earth exchanged supports favours the bifunctional (acid/metallic) character of these catalysts.

In Fig. 6 the evolution of the catalytic activity of each catalyst along the reaction time is represented. In the case of alkali exchanged samples, conversion values decrease as the cation size increases. Under these experimental conditions Pt/Csβ and Pt/KL catalysts show very low catalytic activity (conversion values $\approx$5%), compared with other Pt/Mβ catalysts. In order to increase the conversions, the catalytic performance of both Pt/Csβ and Pt/KL catalysts was also evaluated for lower WHSV (Fig. 6c). Even under these experimental conditions Pt/Csβ shows the lowest conversion value and for Pt/KL the initial conversion is about 50%. However, both catalysts are quickly deactivated. The decrease of activity is more significant for Pt/Csβ (Fig. 6c) with respect to the other catalysts of this series (Fig. 6a). In the case of alkali-earth exchanged catalysts (Fig. 6b), a slight difference is observed in their initial catalytic activity, but this difference increases with the time on stream, due to the different deactivation rates of both catalysts.

The influence of Pt content on the catalytic activity was evaluated by preparing two Pt/Naβ catalysts with different Pt content, 0.5 and 0.2% (the same Pt concentration as in Pt/Csβ). No significant differences are observed in the initial conversion values (Fig. 7), but the deactivation rate increases strongly for the catalyst with the lowest Pt content.

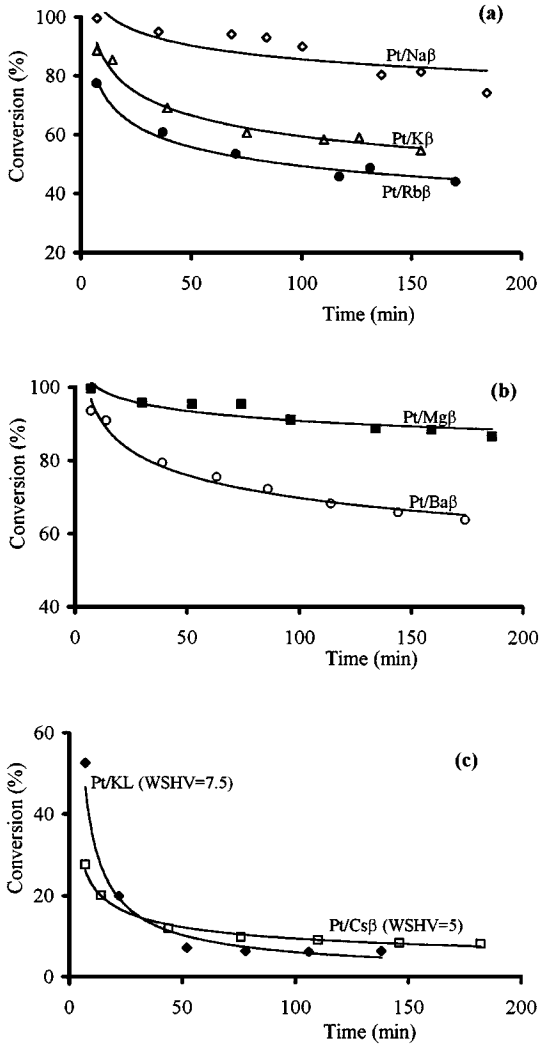

FIG. 6. Conversion of *n*-heptane on Pt/Mβ catalysts at $T = 450^{\circ}$C, $H_2/C_7 = 6$ as a function of the reaction time (a) Pt(0.5%)/Naβ, Pt/Kβ, and Pt/Rbβ at WHSV = 15 h^{-1}, (b) Pt/Mgβ and Pt/Baβ at WHSV = 15 h^{-1}, (c) Pt/Csβ at WHSV = 5 h^{-1} and Pt/KL at WHSV = 7.5 h^{-1}.

Some results about the selectivities observed for the several catalysts after 7 min and 150 min on stream are reported in Table 3. In view of the great differences of activity between the catalysts, even after some changes of operating conditions leading to boundary conditions for the weight of the catalyst and the spacial velocity, it is difficult to compare the selectivity values at isoconversion. However, from the analysis of the table we can observe that for all the catalysts at high conversion the main reaction was cracking, followed by aromatization reaction. The most significant point to emphasize is the high value of aromatics selectivity, found even at lower conversion (27.6%) for Pt/Csβ catalyst, which is comparable to the one observed for Pt/KL zeolite at higher conversion (52.6%). Comparing the ratios (C_7/C_{150}) calculated with the conversion values observed at initial time ($t = 7$ min) and after 150 min on stream, we confirm the different rates of deactivation already mentioned above for the several catalysts, depending on the exchanged cation.

The catalytic activity in reforming reactions is related to the reaction time by a power-law (23, 24). Kooh *et al.* (23) found that the heptane consumption rate on Pt/KBaL catalyst falls proportionally to the −0.22 power of time (at 450°C, 0.16 atm heptane, 0.95 atm H_2, and 6.7 atm He, 240 mL/min flow rate). In our case, the variation of the heptane conversion with the reaction time was also fitted using a power law ($X_{(\mathrm{mol}\%)} = A\,t^{-b}$), which corresponds to the solid lines included in Figs. 6 and 7. The power-law equation fitted for the different catalysts are listed in Table 4. The values of the parameter *b* (power of time) are similar to those presented by Kooh *et al.* (23) and they vary proportionally to the cation size exchanged on the support, ranging between −0.10 for Pt/Naβ and −0.18 for Pt/Rbβ catalysts. Similar results were observed in the alkali-earth catalysts series in which *b* varies from −0.04 in the case of Mg sample to −0.12 for the Ba one. The highest values of the *b* parameter were observed for Pt/Csβ and Pt/KL catalysts (WHSV = 5 and 7.5 h^{-1}, respectively). The deactivation rate is clearly a function of the Pt content, *b* increasing as the Pt content decreases. Pt itself helps to clean active metal sites, as well as the acid sites that are closer to the metallic particles. However, comparing Pt(0.2%)/Naβ ($b = -0.27$) with Pt/Csβ ($b = -0.40$), which present identical Pt content, it is notorious that the deactivation rate also increases as the cation size increases. As previously mentioned, the porous and acidic characteristics of the supports tend to the KL ones as the size of the exchanged cation becomes greater. Furthermore, the catalytic performance also tends to a similar behaviour, decreasing conversion and increasing the deactivation rate. Those facts are especially relevant in the case of Cs. For the Ba-exchanged catalyst this behaviour is not so pronounced, due to its greater acidity, and moreover,

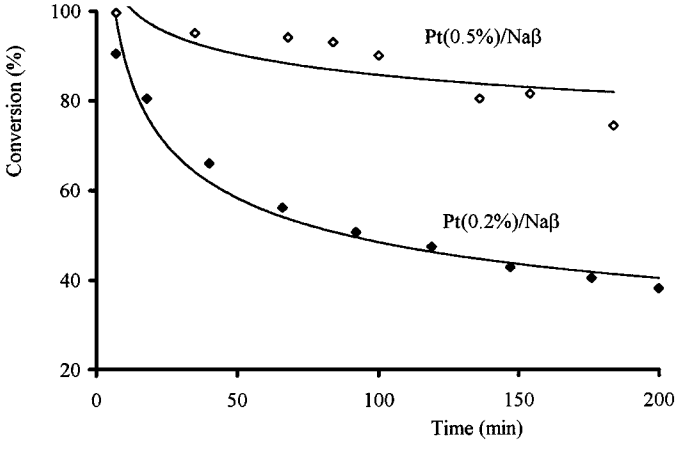

FIG. 7. Conversion of *n*-heptane on Pt(0.2%)/Naβ and Pt(0.5%)/Naβ catalysts at $T = 450^{\circ}$C, $H_2/C_7 = 6$, and WHSV = 15 h^{-1} as a function of the reaction time.

TABLE 3

Conversion and Product Distribution Observed during *n*-Heptane transformation at $T = 450^{\circ}C$, $H_2/nC_7 = 6$

		$t = 7$ min				$t = 150$ min				
Sample	WHSV (h^{-1})	Conv. (%)	Sel. crack. (%)	Sel. isom. (%)	Sel. arom. (%)	Conv. (%)	Sel. crack. (%)	Sel. isom. (%)	Sel. arom. (%)	C_7/C_{150}[a]
Pt/Naβ	15	99.6	80.2	1.3	18.5	81.5	59.3	25.2	15.5	1.2
Pt/Kβ	15	88.6	52.6	17.0	30.4	54.7	27.6	52.4	20.0	1.6
Pt/Rbβ	15	77.5	40.1	38.5	21.4	44.2	19.1	65.5	15.4	1.8
Pt/Csβ	5	27.6	10.6	55.2	34.2	8.3	0.0	65.5	34.5	3.3
Pt/Mgβ	15	99.5	91.3	0.2	8.5	88.4	84.5	7.0	8.5	1.1
Pt/Ba	15	93.5	76.3	10.0	12.6	65.9	45.7	38.7	8.6	1.4
Pt/KL	7.5	52.6	45.9	15.8	38.3	6.4	4.7	75.5	19.8	8.2

[a] Ratio conversion at $t = 7$ min/conversion at $t = 150$ min.

the diffusional problems are not as strong as in the case of Cs, as was shown in Fig. 2. Considering the literature data concerning the stability of Pt/KL in absence of sulphur (12, 25), the great deactivation rate observed for Pt/KL was not expected. From Table 3 we also observe an excessive cracking selectivity for this catalyst, which can indicate the presence of some acidity on the catalyst, favouring the coking reactions, and consequently the fast deactivation of Pt particles that are located in the accessible positions of the pore mouths, as discussed previously. Furthermore, another factor that can affect the expected catalytic activity is the method used for the Pt introduction in KL zeolite that in our case was an ionic exchange, and it is known that with this zeolite the best Pt dispersions are obtained by impregnation (22, 26). The low hydrogen pressure used during reaction also could be a potential complicating factor for the deactivation of Pt/KL zeolite in this study, as verified by other authors (23).

(c) Coke Deposition

During the *n*-heptane reaction, coke deposition takes place. XRD experiments showed that no loss of crystallinity occurs during the reaction and no peaks of graphitic coke ($d = 3.45$ Å) were found. The coke contents on used supports and catalysts were analysed by TG. Naβ support presents, after 3-h reaction, 1.3% of coke and the other supports of this series do not present appreciable coke deposition, because as mentioned above, no activity was detected. In the case of alkali-earth exchanged zeolite, Mgβ presents 8.1% of coke and Baβ 3.4%. The coke contents of used Pt catalysts are also included in Table 4. It is noteworthy that, although Pt/Naβ shows the lowest deactivation rate among the alkali exchanged catalysts, it presents the greatest amount of coke, while Pt/Csβ that presents the maximum deactivation rate does not produce coke during the reaction, or the quantities are only traces which are below detection limits of the thermogravimetric technique used to determine the coke content. Similar results were also observed for alkali-earth exchanged catalysts, in which the coke percentage decreases from 10.0 for a Mg sample to 6.5 in the case of the Ba one. No significant differences on the amount of coke were observed changing the Pt loading on Pt/Naβ catalyst. Pt/KL also does not present coke formation, and once again, these results confirm the similar behaviour of Pt/KL and Pt/Csβ and are in agreement with those exposed by Iglesia *et al.* (12). For catalysts exchanged with smaller cations, coke has a moderate deactivating effect, and the coke depositions are favoured by both the greater acidity and more open porosity (6, 7). The greater deactivation rate of the catalysts exchanged with greater cations, suggests the possibility that deactivation occurs through pore blockage and limitations of the access to the active sites. The first coke molecules (or precursors) formed in the pore mouth near the outer surface are retained because of their low volatility. One coke molecule is enough to inhibit the diffusion of the reactant to the active sites of the channel (7). Coke has therefore a great deactivating effect. The deactivation will be faster and the deactivating effect of coke more pronounced in the supports having steric constraints that tend to the monodimensional pore structure of KL zeolite.

TABLE 4

Coke Contents and Deactivation Power-Law Equations Fitted for Different Catalysts after *n*-Heptane Reaction (at 450°C, $H_2/C_7 = 6$)

Catalyst	WHSV (h^{-1})	Coke[a] (wt.%)	Equation
Pt(0.5%)/Naβ	15	9.9	$X(\%) = 138\ t^{-0.10}$
Pt/Kβ	15	5.8	$X(\%) = 125\ t^{-0.16}$
Pt/Rbβ	15	2.5	$X(\%) = 111\ t^{-0.18}$
Pt/Csβ	5	0.0	$X(\%) = 55\ t^{-0.40}$
Pt/Mgβ	15	10.0	$X(\%) = 110\ t^{-0.04}$
Pt/Baβ	15	6.5	$X(\%) = 122\ t^{-0.12}$
Pt(0.2%)/Naβ	15	8.9	$X(\%) = 165\ t^{-0.27}$
Pt/KL	7.5	0.0	$X(\%) = 208\ t^{-0.77}$

[a] Coke content determined after 3 h time on stream.

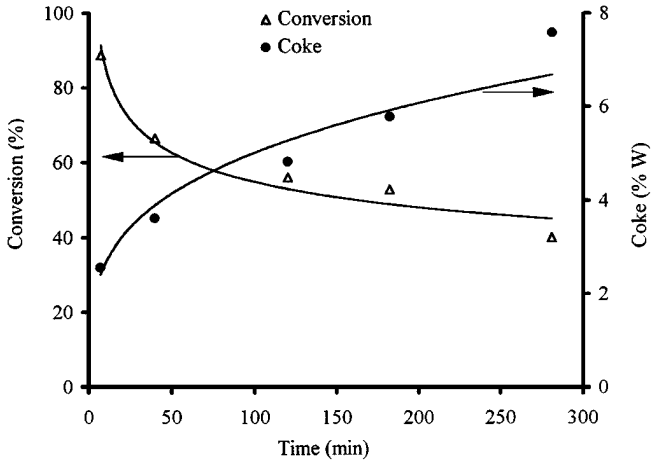

FIG. 8. Relationship between deactivation and coke deposition rates for Pt/Kβ catalyst on *n*-heptane reactions at $T = 450°C$, and WHSV = 15 h^{-1}.

The coke deposition rate (at 450°C, WHSV = 15 h^{-1}, and $H_2/C_7 = 6$) was also studied in the Pt/Kβ sample by stopping the reaction at different run times and determining the coke by TG. The obtained results are shown in Fig. 8. Coke deposition and conversion values show the opposite tendency. The poisoning effect of the coke is stronger during the first minutes of reaction and the amount of coke is 2.6% after 7 min on stream, which suggest a rapid coke deposition and catalyst deactivation on the reaction beginning. The coke percentage increased to 3.6% after 40 min of reaction, and simultaneously conversion values decreased from 90 to 60%, both parameters progressing much slower at higher times on stream.

Different experiments were carried out in order to estimate the effect of coke on chemical and porous characteristics. In Fig. 9, cyclohexane adsorption results of fresh and coked catalysts are compared. The adsorption capacity and adsorption rate decrease strongly in the case of the used

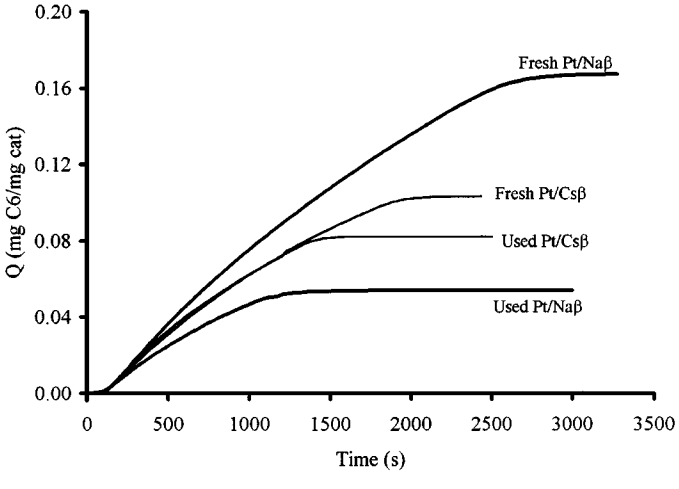

FIG. 9. Adsorption of cyclohexane on fresh and used catalysts.

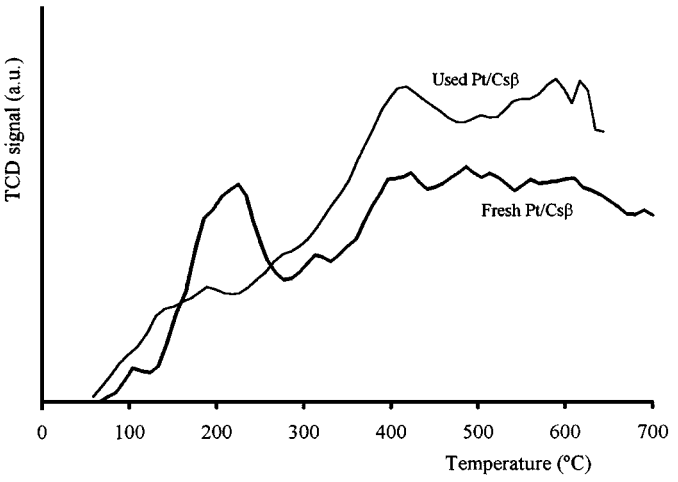

FIG. 10. TPR profiles of fresh and used Pt/Csβ catalyst.

Pt/Naβ catalyst, which presents the highest coke content of the alkali series. However, despite no coke being found on Pt/Csβ, a loss of adsorption capacity of this catalyst is also produced during the reaction.

Changes in the Pt distribution for Pt/Csβ after reaction were analysed by H_2 TPR (Fig. 10) and the particle sizes were determined by TEM (Fig. 11). The used Pt/Csβ was treated in air flow at 325°C for 1 h, attempting to reoxidize the Pt particles, cooled to room temperature and purged in Ar flow for 2 h, and then reduced in Ar/H_2 flow at 10°C/min. Comparing the TPR profiles of fresh and used Pt/Csβ catalyst, it is noteworthy that the first maximum located at 200°C decreases with respect to the second ones, a clear maximum appears at about 400°C, which could indicate that some of the Pt particles located in more accessible positions moved to inner pores. On the other hand, analysing the histogram of Fig. 11 that compares the distribution of Pt particles between fresh and used catalyst, we do not find significant sinterization of the particles after the catalyst Pt/Csβ had been submitted to reaction under the conditions previously

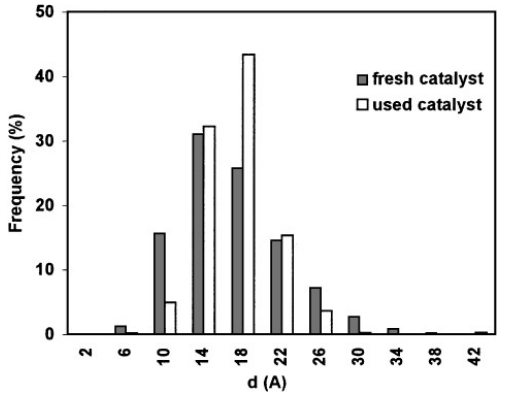

FIG. 11. Size distribution of platinum particles obtained by transmission electron microscopy on fresh and used Pt/Csβ catalyst.

described. These results indicate that the deactivation of the Pt/Csβ catalyst cannot be attributed to metal sinterization. It seems that the main reason for deactivation of this catalyst is the formation during the reaction of a very small amount of organic molecules (coke), which is also justified by the slightly porous blockage found by cyclohexane adsorption (Fig. 9) in used Pt/Csβ. However, the effect of coke deposition does not depend only on the porous blockage that it provokes. The used Pt/Naβ presented a greater porous blockage, and generated many more coke deposits than Pt/Csβ, but despite both these factors and contrarily to Pt/Csβ it showed high catalytic activity after 3 h of reaction. The moderate acid sites existing in Pt/Naβ, responsible for its higher activity, and their proximity to the metallic particles dispersed throughout the crystals promote the growth of coke deposits to a large extent. The greater acidity and number of metallic sites, and the absence of diffusion constraints, makes the catalyst exchanged with Na less sensitive to coke deposits than that exchanged with Cs.

The effects produced by the several cations in the porosity and diffusion properties, in acidity, metal content, or localization of metal particles, jointly contributed to the differences of deactivation rates observed for each catalyst. Different processes can improve the deactivation rate for catalysts exchanged with larger cations. The presence of small amounts of carbonaceous compounds (coke) in the zeolite channels can difficult the diffusion of reactants or products. Furthermore, the small Pt particles located in the pore mouth or on the external surface of the catalyst, become fouled much faster than those inside the zeolite. These latter platinum particles, in the case of catalysts containing larger cations, practically do not contribute to the catalytic activity due to existent diffusional limitations, and the rapid drop of activity is perfectly understandable. So that, on this type of catalyst, the role of these external Pt particles on the reaction mechanism can be very important. As previously indicated (23, 27), fouling by coke deposition of Pt/KL catalyst could take place by decomposition of *n*-heptane on the external Pt crystallites, this coke spreads out over the zeolite surface and blocks the pores, rendering it difficult for heptane to reach the internal platinum clusters.

(d) Some Considerations about the Coke Formation and Its Nature

TG experiments were carried out to determine coke content. DTG profiles are also appropriate to compare coke stability, but DSC curves associated to coke burning provide interesting results and are more sensible than the DTG. The differences in the burning temperature point out differences in the coke nature. The reactivity of the coke is related to its composition, being less aromatic and more reactive as its H/C (hydrogen-to-carbon) ratio increases (7, 28).

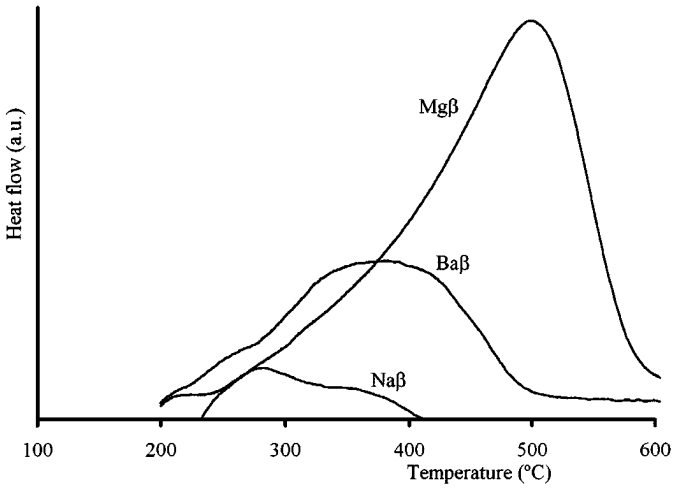

FIG. 12. Heat flow profiles obtained burning the coke deposited on Naβ, Mgβ, and Baβ supports after 2 h of *n*-heptane reaction at 450°C, WHSV = 15 h^{-1}, and $H_2/C_7 = 6$.

Unfortunately, in this work we did not analyse the coke elemental composition by conventional techniques. Moreover, the composition of the coke on the various zeolites must be compared for identical coke contents rather than for identical times on stream (7). Despite these experimental limitations, some interesting conclusions can be taken from the analysis of the heat flow profiles obtained during coke burning.

Figure 12 shows the DSC profiles obtained burning the coke deposited on Mβ supports containing different coke contents. The coke deposited on Naβ support (%C = 1.3) was gasified at low temperatures and the curve shows a maximum below 300°C. In the case of alkali-earth exchanged supports this maximum is shifted to higher temperatures for Baβ (%C = 3.4) it appears about 370°C and for Mgβ (%C = 8.1) at 500°C. These differences in the DSC profiles are certainly due to the different coking loads, which were provoked by the different acidity of the support, as already reported.

According to the results exposed by Guisnet (7) the coke composition depends on the zeolite and for a given zeolite it changes with the coke content. The hydrogen-to-carbon ratio decreases with increasing time on stream, i.e. when the coke content increases, and generally for low coke contents coke is nonaromatic. In our case similar results were observed in Fig. 13, when the coke burning was analysed for the Pt/Kβ catalyst after different reaction times. During the first minutes of reaction it deposited an important amount of coke. The heat flow profile obtained for coke after 7 min of reaction shows clearly two maxima, the first located at 300°C and a second one at about 450°C, the first maximum being slightly more important than the second one. As the reaction time increases, the coke content increases and becomes more stable. Both maxima are progressively shifted to higher temperatures and the second maximum becomes

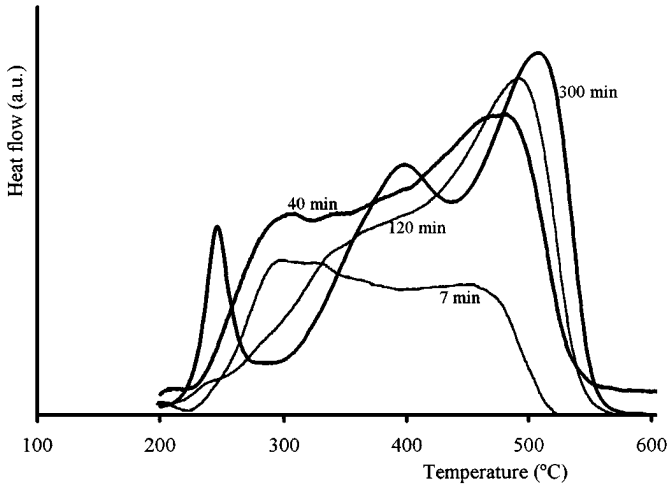

FIG. 13. Heat flow profiles obtained when the coke burning was analysed for Pt/Kβ catalyst after different reaction times on *n*-heptane transformation at 450°C, WHSV = 15 h^{-1}, and $H_2/C_7 = 6$.

more important, the first one being progressively masked. Special mention must be made of the heat profile obtained by burning the coke after a run developed during 5 h, which generated a coke content of 7.6%. Three peaks corresponding to different types of coke are perfectly defined in this profile, a new one at a lower temperature (250°C) and the other two at 400 and 550°C. These latter peaks correspond to the ones observed for the runs performed with lower times of reaction, but that have been displaced progressively with the increase of the time of reaction and, obviously, due to the growth of coke deposits. The analysis of these results as a function of the coke content, leads to the conclusion that for low times of reaction, the coke that is present in a small amount is formed preferentially on the acid sites more distant from the Pt particles and its oxidation is slightly difficult. The coke removal gets more difficult with increasing coke content, but when the coke content is growing and reaches higher values, it begins to spread very close to, or cover the metallic particles, and in this case the oxidation becomes easier. The peak observed at the lower temperature (250°C) can be assigned to the combustion of the coke deposited over or close to the Pt particles, which act as a combustion accelerator as has been found (29, 30) for conventional bifunctional reforming catalysts (Pt/Al_2O_3). The progressive increase of the maximum temperature of the peaks located at higher temperatures can be attributed to changes of the coke composition as a function of time on stream and, also, to the diffusional limitations of oxygen due to the blockage of the pores by the highly polyaromatic carbonaceous compounds. Magnoux *et al.* (31) verified that coke oxidation is a shape-selective process, and differences in the mode of contact between oxygen and the less accessible coke molecules can explain the differences in coke oxidizability.

Comparing the heat flow profiles shown in Fig. 14 for Pt/Naβ with different Pt loading, it is notorious that the curves are similar, but the two peaks at higher temperature assigned to the combustion of coke deposited on acid sites are influenced by the coke content that is greater for the catalyst containing 0.5% of Pt. Also in this case the low temperature peak is shifted to lower temperatures because the presence of a great amount of metal makes the oxidation of coke easier.

In order to analyse these catalysts for the influence of the acidity in the process of coke formation, in Fig. 15a we compare the two Pt catalysts exchanged with the smallest cations (Na, Mg) that generated similar coke contents after 3 h of reaction (see Table 4) and that showed great differences of acidity of the support. The range of temperatures obtained for the complete removal of coke is similar, but the composition and/or the localization of coke is different. Pt/Naβ presents two well-resolved peaks at lower temperatures (250 and 400°C) that show the presence of a type of coke that is less dehydrogenated and more reactive. In the case of the Pt/Mgβ catalyst, the most acidic support, the first two peaks are masked in the tail of the high temperature peak and are assigned to the coke formed in the more distant acid sites of Pt particles. This can be explained assuming that the coke is preferentially deposited over the acid sites, and while Pt/Mgβ have a great number of acid sites dispersed inside the pores, in Pt/Naβ the number of acid sites is more reduced; moreover, the main part of them was created during the activation of Pt, so it is normal that they were placed close to the Pt particles and, consequently, the growth of coke is forced directly to these particles. It would be interesting to extend the time of reaction with Pt/Mgβ catalyst for more than 3 h and to analyse the evolution of the corresponding heat profile. Unfortunately we do not have

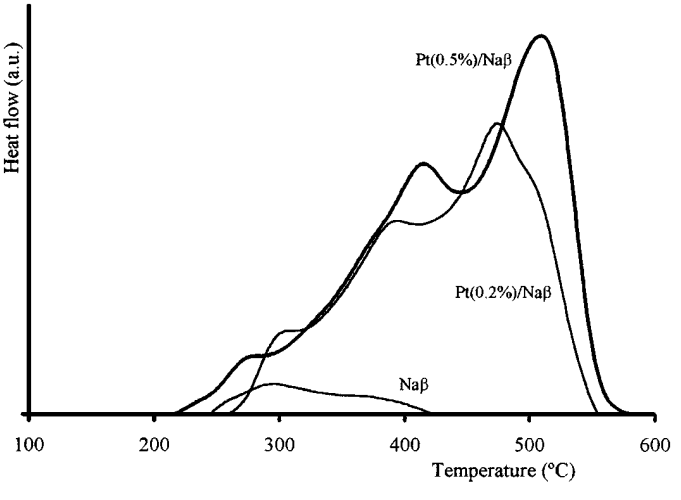

FIG. 14. Heat flow profiles of coke burning on Naβ support and Pt/Naβ catalysts with different Pt content. The coke deposition had occurred after 2 h of *n*-heptane reaction at 450°C, WHSV = 15 h^{-1}, and $H_2/C_7 = 6$.

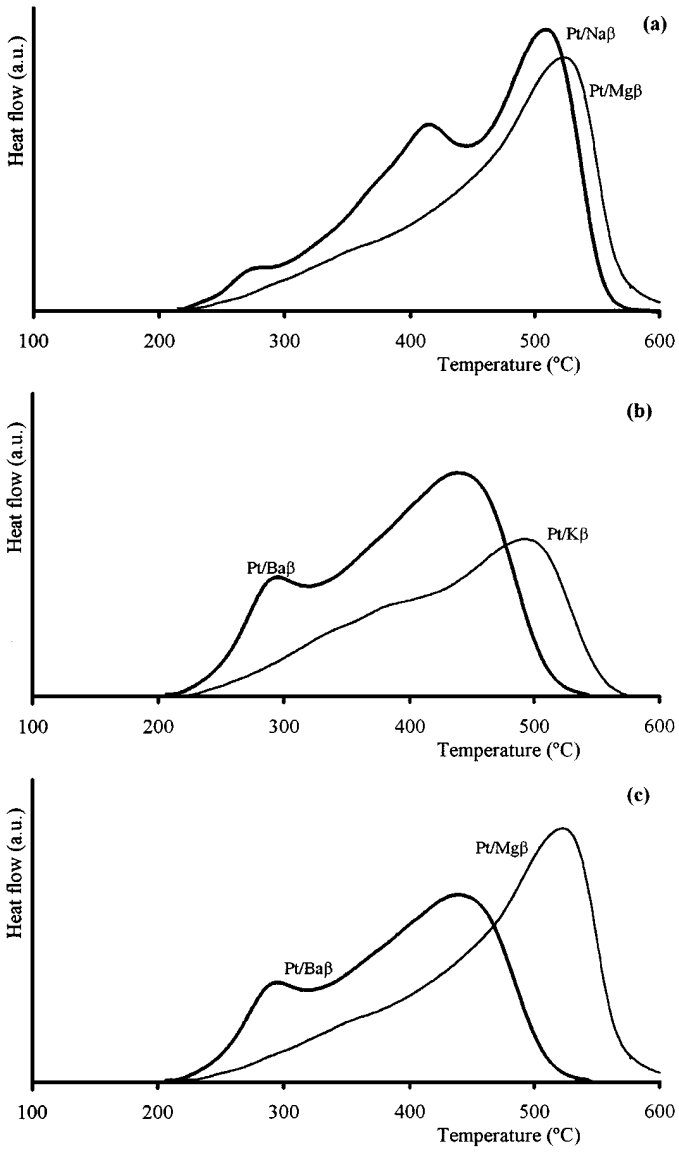

FIG. 15. Comparison of heat flow profiles obtained burning the coke deposited on (a) Pt/Mgβ and Pt/Naβ catalysts, (b) Pt/Baβ and Pt/Kβ catalysts, (c) Pt/Mgβ and Pt/Baβ catalysts.

those results, but probably the trend would be to increase the more reactive coke corresponding to the peaks at low temperature, because the increasing coke would tend to get progressively closer to the metallic sites. The importance of acidity of the support is remarkable in this catalyst, leading to the formation of a very stable single type of coke, either with or without Pt in the catalyst, as can be observed by comparing the support heat profile in Fig. 12 (Mgβ with 8.1% coke) and the one corresponding to the Pt/Mgβ catalyst (10% coke). Once more the peak located at about 500°C increased and was shifted to a slightly higher temperature as a consequence of the amount of coke deposited.

The results reported in Figs. 15b and c allow the analysis of the influence of the size of cation in the coke nature. Figure 15b displays the DSC profiles of coke burning for catalysts containing alkali and alkali-earth cations of different sizes (K and Ba), but containing similar coke contents, and Fig. 15c shows the profiles corresponding to the catalysts with alkali-earth cations (Mg, Ba) with distinct coke contents and acidity. In both comparisons Pt/Baβ shows the maximum of the second peak shifted to about 100°C lower temperature. The low temperature peak (at about 275°C) is also more salient than for Pt/Kβ or Pt/Mgβ. The differences obtained between the catalyst exchanged with Ba and the others containing smaller cations (Mg and K) can be explained, taking into account that the Ba exchange provoked a reduction of the channel dimensions or even a porous blockage, and all these transformations have been accountable for the changes in the loading and localization of Pt and for the low activity and coke content (compared to Mgβ). In this sense, it is evident that the presence of Ba in the catalyst limits both the diffusions of the reactants to the inner pores of the crystallites and the growth of coke deposits. Furthermore, contrary to the other catalysts containing K and Mg, a great part of Pt particles in the Pt/Baβ catalyst is located close to or over the external surface. It means that the production of coke is confined to a region where the acid sites are placed near the Pt particles, and their hydrogenating effects inhibit the production of highly dehydrogenated compounds, making the coke more stable. This factor explains not only the reduction of the temperature required for complete removal of the coke on Pt/Baβ, but also the evidence of the peak at about 275°C, characteristic of a less dehydrogenated and more reactive coke.

It is important to point out that the influence of the cation size on porous textures and consequently on coke deposition is also affected by the differences of acidity observed in the several supports and catalysts. For example, Naβ and Mgβ supports showed similar adsorption characteristics, but the observed coke nature is completely different (Fig. 12). Furthermore, if we compare Pt/Csβ and Pt/Baβ catalysts both with diffusional limitations, in the first the coke content was not measurable, but an important amount of coke was found in Pt/Baβ, and its combustion was easier than in the other catalysts exchanged, either with alkali or alkali-earth cations.

All the results showed in this study for Pt/Csβ catalyst attest to its particular properties which are very similar to Pt/KL. Jointly with all the effects above-mentioned, accounting for this behaviour are also the strongest Pt–zeolite interactions that were found in this catalyst and that will be discussed in another publication (32).

(e) Catalyst Regeneration

Catalyst regeneration is generally carried out through removal of coke under oxidative conditions. The preservation of the catalyst properties during reactivation is of critical importance; the process must be monitored carefully in order

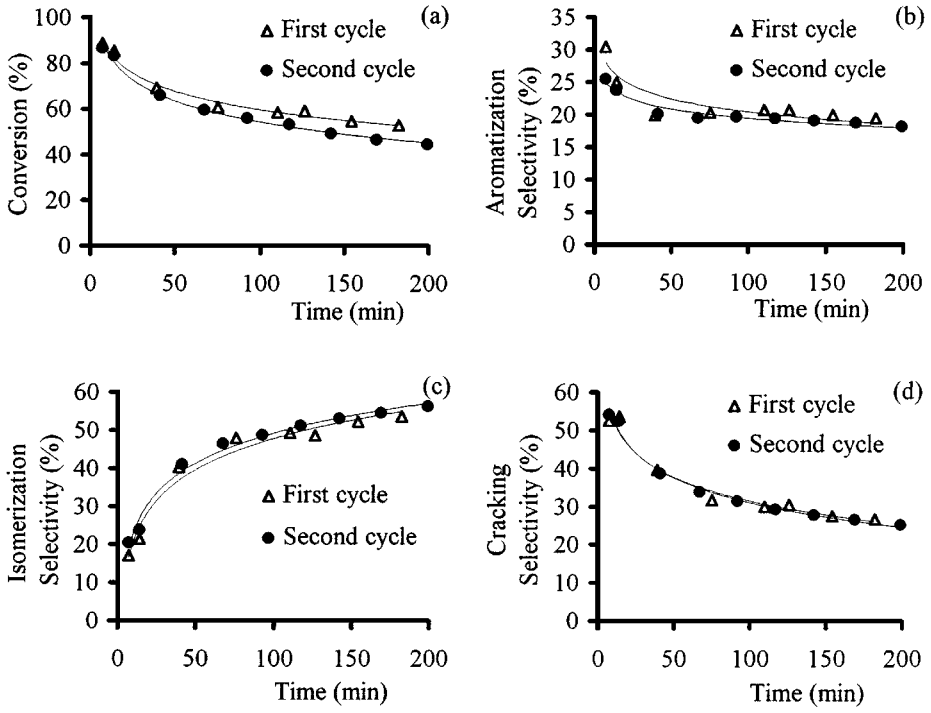

FIG. 16. Evolution of *n*-heptane conversion and selectivities of aromatization, isomerization, and cracking for Pt/Kβ catalyst: fresh (first reaction cycle) and after 3 h of reaction followed by regeneration (second reaction cycle).

to ensure that predetermined temperature limits are not exceeded, the temperature control being achieved by regulation of the oxygen content (6, 33). In our case, regeneration of the Pt/Kβ catalyst was carried out by burning the coke in air flow (1 mL/s) at 425°C for 1 h. Previous experiments performed in the thermobalance showed that below 350°C the coke gasification rate (coke was heated at this temperature under N_2 flow and then was changed for air flow) is extremely low, as expected on the basis of the larger amount of coke that is gasified at 500°C. So, 425°C seems to be an adequate temperature, taking into account the exothermicity of the combustion; keeping the sample at this temperature for 1 h, the removal of coke is practically complete. Under these conditions we also prevent the Pt sinterization, which is promoted mainly above 500°C (11). In fact, when, after 3 h of reaction, the catalyst Pt/Kβ was regenerated under the operational conditions described above, it recovered its initial conversion with identical product distribution (Fig. 16). The amount of coke deposited during the second reaction cycle (6.2%) and the heat flow profile are similar to those observed during the first ones. The regeneration of the chemical and catalytic properties of Pt/Kβ catalyst is fully recovered after this treatment.

CONCLUSIONS

The chemical and catalytic properties of Pt/Mβ catalysts are strongly influenced by the characteristics of the support. Either for alkali or alkali-earth catalysts, as the cation size increases the support acidity decreases, the adsorption capacities decrease, and the characteristics of the catalysts tend to those showed by the KL zeolite. In the case of alkali cations, the catalytic activity of the support is negligible for *n*-heptane reactions, only providing slightly the double bond isomerization of 1-butene to *cis*- and *trans*-2-butene. However, greater acidity and stronger acid sites present on alkali-earth supports provide the skeletal isomerization of 1-butene to *iso*-butene and a high catalytic activity on *n*-heptane reactions.

The catalytic activity of Pt/Mβ catalysts decreases in both series as the cation size increases and greater differences are observed in the case of the Pt/Csβ catalyst that presents a catalytic behaviour similar to the Pt/KL catalyst. The deactivation rate is faster and the deactivating effect of coke more pronounced in the catalysts exchanged with larger cations, due either to the observed porous blockage or to the lower Pt content obtained for these catalysts. For catalysts exchanged with smaller cations, coke has a moderate deactivating effect, and the coke depositions are favoured by both the greater acidity and more open porosity. The less porous and nonacidic Pt/Csβ and Pt/KL catalysts do not produce appreciable amounts of coke but show the highest deactivation rates. In these two catalysts a part of the Pt particles is located close to or on the external surface, and very small amounts of coke are enough to deactivate these particles and totally block the pores, rendering

it difficult for heptane to reach the internal platinum clusters.

Coke deposited on alkali and alkali-earth Mβ zeolite, during the *n*-heptane transformation, is burnt at progressively higher temperatures as the support acidity increases, and the most acidic support (Mgβ) produces the most stable coke that probably is more aromatic.

The localization of Pt particles and their proximity to the acid sites influences the coke nature and its subsequent removal. The coke is formed preferentially on the acid sites more distant from the Pt particles and its oxidation is difficult. In the catalysts without steric constraints, when the coke content increases, or in the catalysts with steric constraints in which the formation of coke is confined to the pore entrances and external surface, the coke begins to spread very close to or over the metallic particles, and its oxidation becomes easier.

After regeneration of Pt/Kβ by burning the coke under air flow, Pt properties are not modified and identical conversions, product distribution, amount, and types of coke were obtained.

ACKNOWLEDGMENTS

Support of this work by EC, HCM network Contract ERB CHRX CT 940477 are gratefully acknowledged. The authors thank Dr. M. Kermarec (P. et M. Curie University-Paris) for obtaining the transmission electron micrographs, and Dr. P. Magnoux for helpful discussions of this work.

REFERENCES

1. Allum, K. G., and Willians, A. R., *Stud. Surf. Sci. Catal.* **36**, 691 (1988).
2. Querini, C. A., and Fung, S. C., *J. Catal.* **161**, 263 (1996).
3. Chen, N. Y., and Garwood, W. E., *J. Catal.* **52**, 453 (1978).
4. Marecot, P., Akhachane, A., and Barbier, J., *Catal. Lett.* **36**, 37 (1996).
5. Neuber, M., Ernst, S., Geerts, H., Grobet, P. J., Jacogs, P. A., Kokotailo, G. T., and Weitkamp, J., *Stud. Surf. Sci. Catal.* **36**, 567 (1988).
6. Bibby, D. M., Howe, R. H., and McLellan, G. D., *Appl. Catal.* **93**, 1 (1992).
7. Guisnet, M., and Magnoux, P., *Appl. Catal.* **54**, 1 (1989).
8. Derouane, E. G., *Stud. Surf. Sci. Catal.* **20**, 221 (1985).
9. Sinfelt, J. H., *in* "Catalysis, Science and Technology" (J. R. Anderson and M. Boudart, Eds.), Vol. 1, p. 257. Springer-Verlag, New York, 1981.
10. Bernard, J. R., *in* "Proceedings 5th International Zeolites Conference" (L. V. C. Rees, Ed.), p. 686. Heyden, London, 1980.
11. Hughes, T. R., Buss, W. C., Tamm, P. W., and Jacobson, R. L., *Stud. Surf. Sci. Catal.* **28**, 725 (1986).
12. Iglesia, E., and Baumgartner, J. E., *in* "Proceedings 10th International Congress on Catalysis, Budapest, 1992" (L. Guczi, F. Solymosi, and P. Tétényi, Eds.), Part B, p. 993. Elsevier, Amsterdam/Akadémiai Kiadó, Budapest, 1993.
13. Smirniotis, P. G., and Ruckenstein, E., *J. Catal.* **140**, 526 (1993).
14. Smirniotis, P. G., and Ruckenstein, E., *Catal. Lett.* **25**, 351 (1994).
15. Smirniotis, P. G., and Ruckenstein, E., *Appl. Catal.* **117**, 75 (1994).
16. Zheng, J., Dong, J. L., Xu, Q. H., Liu, Y., and Yan, A. Z., *Appl. Catal.* **126**, 141 (1995).
17. Kiricsi, I., Flego, C., Pazzuconi, G., Parker, W. O., Millini, R., Jr., Perego, C., and Bellusi, G., *J. Phys. Chem.* **98**, 4627 (1994).
18. Zheng, J., Dong, J. L., and Xu, Q. H., *Stud. Surf. Sci. Catal.* **84**, 1641 (1994).
19. Han, W. J., Kooh, A. B., and Hicks, R. F., *Catal. Lett.* **18**, 193 (1993).
20. Blomsma, E., Martens, J. A., and Jacobs, P. A., *J. Catal.* **135**, 141 (1993).
21. Pines, H., and Stalick, W. M., *in* "Base Catalyzed Reactions of Hydrocarbons and Related Compound" (H. Pines and W. M. Stalick, Eds.), p. 26. Academic Press, New York, 1977.
22. Ostgard, D. J., Kustov, L., Poeppelmeier, K. R., and Sachtler, W. M. H., *J. Catal.* **133**, 342 (1992).
23. Kooh, A. B., Han, W. J., and Hicks, R. F., *Catal. Lett.* **18**, 209 (1993).
24. Pacheco, M. A., and Petersen, E. E., *J. Catal.* **86**, 75 (1984).
25. Iglésia, E., and Baumgartner, J. E., *in* "Proc. 9th Int. Zeolite Conference" (R. Von Ballmoos, J. B. Higgins, and M. M. J. Treacy, Eds.), Vol. II, p. 421. Butterworth-Heinemann, London, 1992.
26. Larsen, G., and Haller, G. L., *Catal. Today* **15**, 431 (1992).
27. Han, W. J., Kooh, A. B., and Hicks, R. F., *Catal. Lett.* **18**, 219 (1993).
28. Resasco, D. E., and Haller, G. L., *in* "Catalysis," Vol. 11, Chap. 9. CRC Press, Boca Raton, FL, 1994.
29. Parera, J. M., Figoli, N. S., and Traffano, E. M., *J. Catal.* **79**, 481 (1983).
30. Barbier, J., *in* "Catalyst Deactivation 1987" (B. Delmon and G. Froment, Eds.), p. 1. Elsevier, Amsterdam, 1987.
31. Magnoux, P., and Guisnet, M., *Zeolites* **9**, 329 (1989).
32. Maldonado-Hodar, F. J., Becue, T., Kermarec, M., Massiani, P., Silva, J. M., and Ribeiro, M. F., in preparation.
33. Penick, J. E., Lee, W., and Maziuk, J., *ACS Symp. Ser.* **226**, 18 (1987).